Available online at www.sciencedirect.com

ScienceDirect

Energy Procedia 157 (2019) 1320–1327

Energy Procedia

www.elsevier.com/locate/procedia

Technologies and Materials for Renewable Energy, Environment and Sustainability, TMREES18, 19–21 September 2018, Athens, Greece

Comparative Assessment of the Degradation Behaviour of API 5l X65 And Micro-Alloyed Steels in E20 Simulated Fuel Ethanol Environment

O.O. Joseph[a]*, C.A. Loto[a], O.O. Joseph[b], J.O. Dirisu[a]

[a]*Department of Mechanical Engineering, Covenant University, P.M.B 1023, Ota, Nigeria*
[b]*Department of Mechanical Engineering, Federal University of Technology, P.M.B. 704, Akure, Nigeria*

Abstract

Presently, bio-fuels are evolving as a significant alternative to tackle the problem of global warming in the world. Fuel ethanol is one of such alternatives employed to reduce the usage of fossil fuels such as petrol. Regardless of the great potentials posed by fuel ethanol in comparison to gasoline fuels, corrosion and stress corrosion cracking (SCC) in the presence of fuel ethanol has recently been recognized and identified as a phenomenon in end-user storage and blending facilities. Predictions on the performance of pipeline steels in fuel ethanol environments, are therefore, needed in solving the ethanol SCC problem. Electrochemical tests have been conducted for API 5L X65 and micro-alloyed steel (MAS) in E20 simulated fuel grade ethanol (SFGE) environment via potentiodynamic polarization and mass loss methods. The tests were performed using simulated E20 fuel grade ethanol with additions of 5 volume percent methanol, 1 volume percent water and 32 mg/L NaCl. Mass loss corrosion rates were very low (generally less than 2 mpy). Results show that the two materials are susceptible to degradation in E20 simulated fuel grade ethanol (SFGE). No significant difference was observed in the mass loss corrosion rates of API 5L X65 and micro-alloyed steels in E20 SFGE. However, morphological observation of the post-corrosion samples and calculated polarization resistance show micro-alloyed steel as more compatible with E20 in this regard.

Selection and peer-review under responsibility of the scientific committee of Technologies and Materials for Renewable Energy, Environment and Sustainability, TMREES18.

* Corresponding author.
E-mail address: funmjoseph@gmail.com

Selection and peer-review under responsibility of the scientific committee of Technologies and Materials for Renewable Energy, Environment and Sustainability, TMREES18.
10.1016/j.egypro.2018.11.297

Keywords: corrosion; degradation; E20; SFGE; API 5L X65; micro-alloyed steel

1. Introduction

The corrosive effects of fuel ethanol environments on transport and storage infrastructure necessitates an understanding of the surface and structural integrity of several metallic components utilized in the process [1]. Such components include pipe steels, storage tanks, railcars, ships, amongst others. A previous study [2] revealed micro-alloyed steel to be compatible with E20 (SFGE) at a very low corrosion rate. With E20, dissolved chlorides and high acidity promoted pit initiation and growth in micro-alloyed steel [2]. Furthermore, degradation of the mechanical integrity of ethanol piping and steel tanks is established in literature due to the well-known phenomenon of ethanol stress corrosion cracking [1; 3-6]. A study [7] showed corrosion rates of typically less than 1 mil per year (mpy) for carbon steels in various ethanol environments using coupons and electrochemical methods. However, this study is focused on a comparative assessment of the electrochemical behaviour of X65 steel and micro-alloyed steel in E20 SFGE in order to predict which of the two is most compatible for fuel ethanol service; thereby expanding the body of knowledge in this expanse.

2. Experimental

2.1 Materials

A pipeline steel (API 5L X65) and a micro-alloyed steel plate was used for immersion and electrochemical tests. The X65 pipeline steel (425 mm diameter with 7 mm wall thickness) was obtained from an oil and gas company and the micro-alloyed steel plate (11 mm in thickness) was obtained in as-rolled condition from a steel company. The determined chemical compositions of the steels are shown in Table 1. Representative microstructures of the two steels are also shown in Fig. 1. Micro-alloyed steel consists mostly of ferritic structure with lamellar pearlite arbitrarily distributed in the ferrite matrix. The X65 steel shows a finer-grained structure consisting of polygonal ferrite and lamellar pearlite.

Table 1. Chemical composition of X65 and micro-alloyed steels in as-received condition (wt. %)

Element	C	Mn	Si	Cr	Ni	Al	Ti	Mo	Cu	Fe
API-5L X65	0.08	1.22	0.245	0.022	0.023	0.026	0.0029	0.0062	0.008	balance
MAS	0.13	0.77	0.012	0.027	0.015	0.042	0.0025	0.0017	0.006	balance

2.2 Test Environment

E20 fuel blend was prepared partly in accordance with ASTM D-4806-07 [8] for fuel grade ethanol and as reported in literature [9, 10]. The reagents used for the SFGE environment include: 195 proof ethanol, ultra-pure water (~18 MΩ.cm), glacial acetic acid, pure methanol and pure sodium chloride (NaCl) with purity ›99%. Addition of 80 percent unleaded gasoline to 20 percent SFGE made up E20 fuel blend used for the tests.

2.3 Mass loss and Potentiodynamic Tests

Mass loss and potentiodynamic polarization tests were performed at ambient temperature (27ºC). Test specimens of dimensions 30 x 30 x 11 mm for micro-alloyed steel (replicate number of 2) and 30 x 30 x 7 mm for X65 steel (replicate number of 2) were machined for mass loss tests.

(a)

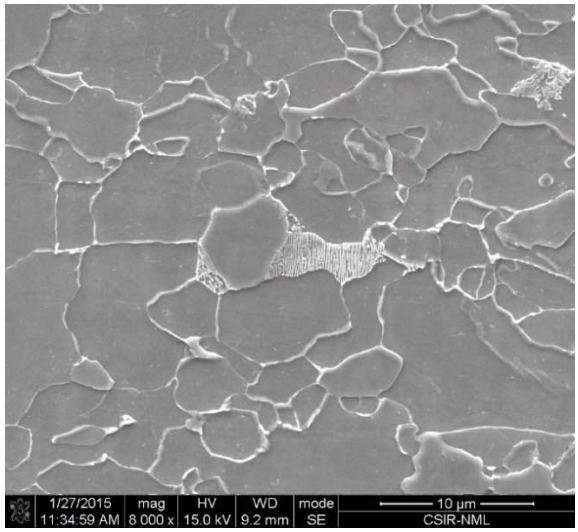

(b)

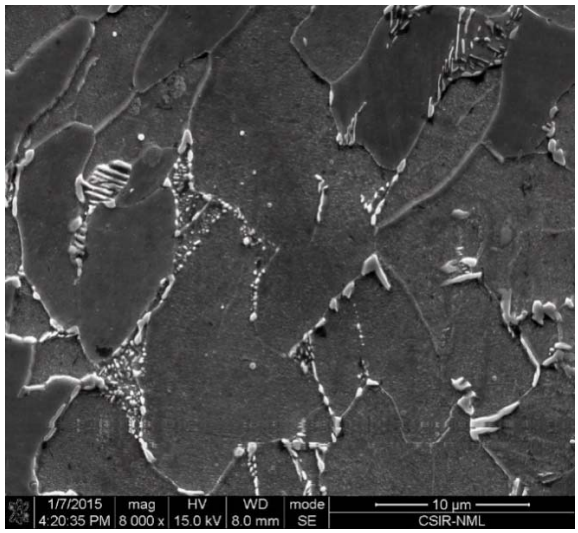

Fig. 1 SEM image of a) API-5L X65 steel and b) MAS in as-received condition.

The immersion test samples were dry-abraded with suspended in air-tight sealed plastic containers containing 300 ml SFGE. Exposure time was for 60 days. Cleaning as per ASTM G1-03 [11] and morphological examination of corroded samples (via a FEI-430 NOVA NANO FEG-Scanning Electron Microscope) was carried out at the end of the exposure period. Furthermore, corrosion rate was calculated in mils per year using equation (1) [10].

$$C.R = \frac{(K \times W)}{(A \times T \times D)} \tag{1}$$

Where K is a constant (534), T is the exposure time in hours, A is the area in square inches, W is the mass loss in milligrams, D is the density in g/cm^3.

For anodic polarization tests, each of the specimens were mounted to reveal an exposed area of 15 x 10 mm^2 after

dry-abrasion with abrasive paper of up to 2000 microns. Duplicate polarization tests were also performed using a Gamry Potentiostat/Galvanostat/ZRA. The test setup was made up of a three-electrode glass cell which consisted of saturated calomel electrode (SCE) as the reference electrode and platinum wire as the counter electrode. The polarization tests commenced with cathodic polarization at -0.75 V vs SCE. A potential scan rate of 2 mV/s was used.

3. Results and Discussion

3.1 Comparison of mass loss and corrosion rates obtained for API 5L X65 and micro-alloyed steels

The bar charts in Figures 2a and 2b show the trend observed for mass loss and corrosion rates determined for both X65 and micro-alloyed steels. X65 steel exhibited highest corrosion rate. However, the margin of rise in corrosion rate from 0.00125 mpy for micro-alloyed steel to 0.00131 mpy for X65 steel is insignificant (approximately 4.8 percent). Consequently, it can be decided that there is no significant difference in the mass loss corrosion rates of the two steels in E20 SFGE. It is important to also note that the determined corrosion rates were very small.

Nevertheless, surface examination (via scanning electron microscope) of the corroded steels after the immersion tests shows significant pitting on the surface of X65 steel in comparison to micro-alloyed steel (Fig. 3). The excessive pitting explains the marginal difference in their corrosion rates. The occurrence of pits in the two steels due to immersion in E20 for the period of 60 days is in agreement with the results of investigations carried out on the corrosion behaviour of carbon steel in E20 as reported in literature [6].

The availability of oxygen and the hygroscopic nature of ethanol have been identified as factors for the participation of ethanol in corrosive reactions [7]. Pitting of carbon steel in SFGE are also associated with water and chloride contents of the fuel [6].

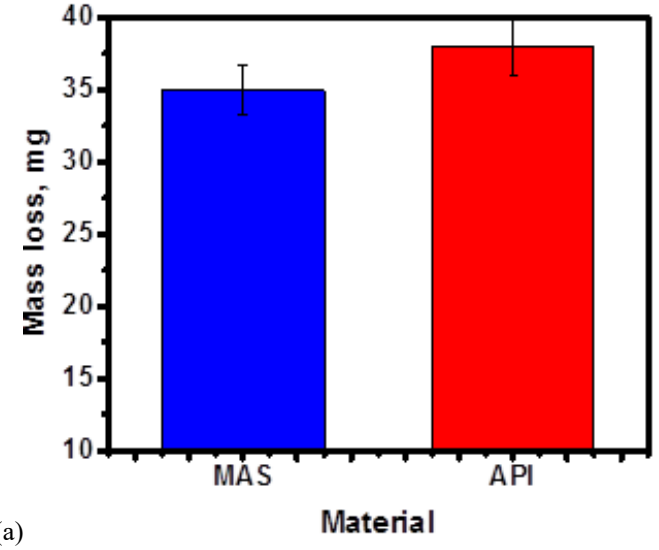

(a)

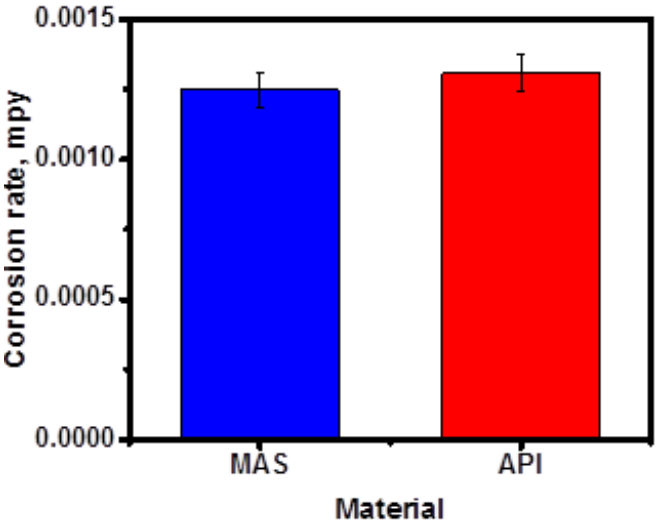

(b)

Fig. 2 Mass loss and corrosion rates of (a) API 5L X65 steel and (b) Micro-alloyed steel.

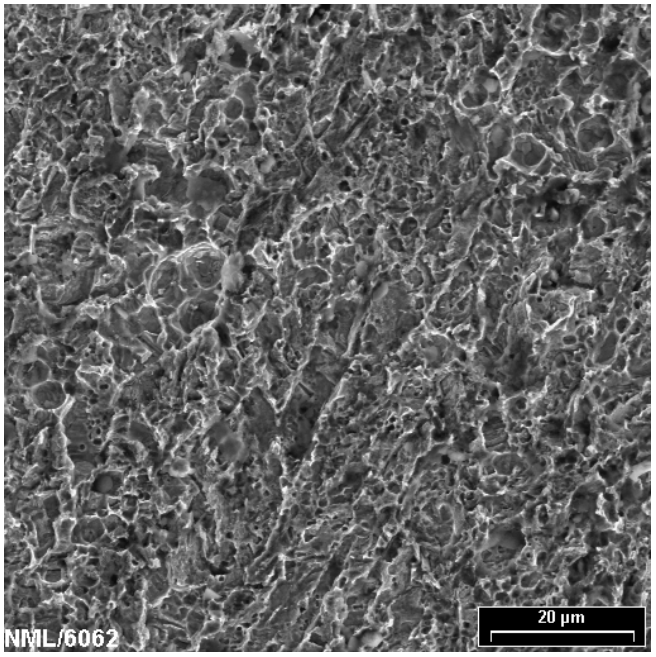

(a)

(b)

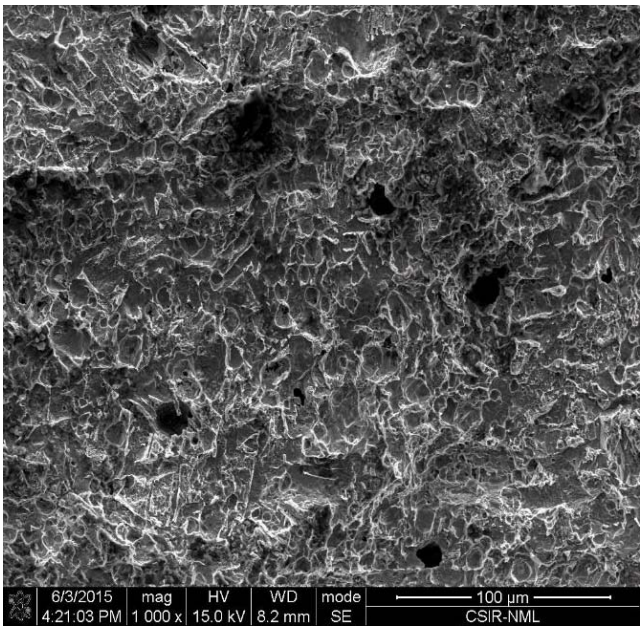

Fig. 3 SEM image of (a) API 5L X65 and (b) micro-alloyed steel at 1000x after immersion in E20 for 60 days.

3.2 Comparison of polarization test results for API 5L X65 and micro-alloyed steels

The results of anodic polarization carried out on the two steels with similar potential difference (1.5 V_{SCE}) from their initial OCPs are shown in Table 2 and Fig. 4. No distinct passivation is seen from the polarization curves. X65 steel show higher $i_{corr\text{-}estimate}$ in comparison to micro-alloyed steel which is consistent with the higher corrosion rate seen from mass loss test in Fig. 2. Furthermore, the polarization resistance (R_p) of the two steels was calculated to determine the degree of their resistance to corrosion using Equation (2) [12]. Table 2 shows that polarization resistance was least for X65 steel which indicates that resistance to charge-transfer reactions was smallest at the surface of X65 steel. This is also a possible explanation for the excessive pitting observed on X65 steel.

$$R_p = \frac{\beta_a \beta_c}{2.3 I_{corr}\left(\beta_a + \beta_c\right)} \tag{2}$$

Where R_p is polarization resistance (ohms), β_a is anodic slope (v/decade), β_c is cathodic slope (v/decade), I_{corr} is current (A/cm^2).

Table 2. Anodic Polarization Data for X65 and micro-alloyed steels in E20

Material	E_{corr} (mv)	$i_{corr\text{-}estimate}$ (A/cm^2)	R_p (Ω)
API 5L X65 steel	-492	2.18 x 10^{-6}	129
Micro-alloyed steel	-445	7.14 x 10^{-6}	443

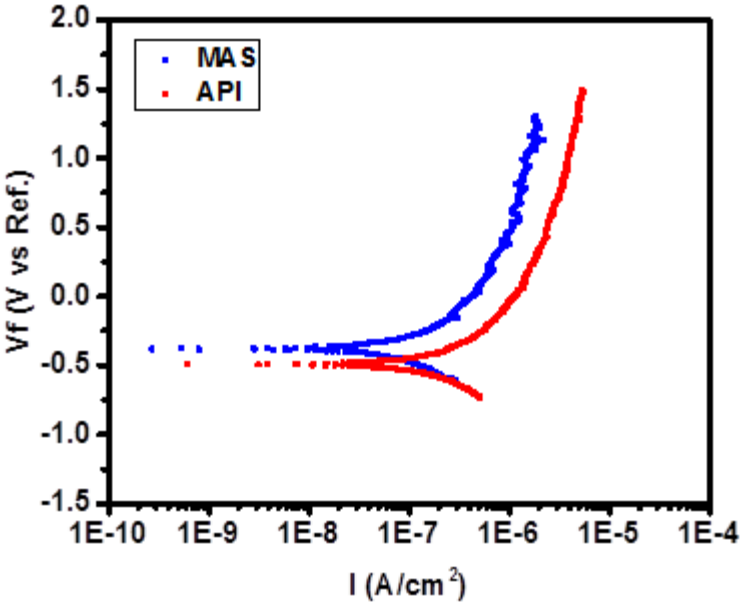

Fig. 4 Typical anodic polarization curves for X65 and micro-alloyed steels in E20 simulated fuel grade ethanol.

6. Conclusions

Based on the study described herein, it can be concluded that there is no significant difference in the mass loss corrosion rates of API 5L X65 and micro-alloyed steels in E20 SFGE. Furthermore, X65 steel show higher $i_{corr\text{-}estimate}$ in comparison to micro-alloyed steel which is consistent with the higher corrosion rate values obtained. Morphological observation of the post-corrosion samples and calculated polarization resistance values show micro-alloyed steel as better suited to E20.

Acknowledgements

This work was co-sponsored by CSIR-National Metallurgical Laboratory, Jamshedpur, India and The World Academy of Sciences (TWAS), Trieste, Italy (FR No. 3240275047). Covenant University is acknowledged for open access funding.

References

[1] Filippini, Massimo, and Lester C. Hunt. "Energy demand and energy efficiency in the OECD countries: a stochastic demand frontier approach." *Energy Journal* 32(2) (2011): 59-80.

[2] Filippini, Massimo, and Lester C. Hunt. "US residential energy demand and energy efficiency: A stochastic demand frontier approach." *Energy Economics* 34(5) (2012): 1484-1491.

[3] Weyman-Jones, Thomas, Júlia Mendonça Boucinha, and Catarina Feteira Inácio. "Measuring electric energy efficiency in Portuguese households: a tool for energy policy." *Management of Environmental Quality: An International Journal* 26(3) (2015): 407-422, doi:10.1109/EMS.2008.12.

[4] Saunders, Harry. "Theoretical Foundations of the Rebound Effect", in Joanne Evans and Lester Hunt (eds) *International Handbook on the Economics of Energy*, (2009) Cheltenham, Edward Elgar

[5] Sorrell, Steve. "The Rebound Effect: definition and estimation", in Joanne Evans and Lester Hunt (eds) *International Handbook on the Economics of Energy*, (2009) Cheltenham, Edward Elgar

[1] Sowards, J.W., Weeks, T.S., Mc Colskey, J.D. "The influence of simulated fuel-grade ethanol on fatigue crack propagation in pipeline and storage-tank steels," *Corros. Sci.,* 75, pp. 415-425 (2013).

[2] Joseph, O.O., Loto, C.A., Sivaprasad, S., Ajayi, J.A. and Fayomi, O.S.I., "Comparative assessment of the degradation mechanism of micro-alloyed steel in E20 and E80 simulated fuel grade ethanol environments," *AIP Conf. Proc.*, 1758, 020019 (2016); doi: 10.1063/1.4959395
[3] Kane, R.D., Sridhar, N., Brongers, M., Beavers, J.A., Agarwal, A.K., Klein, L., "Stress corrosion cracking in fuel ethanol: a recently recognized phenomenon," *Mater. Performance,* 44, pp. 50-55 (2005).
[4] Cao, L., Frankel, G.S., Sridhar, N. "Effect of chloride on stress corrosion cracking susceptibility of carbon steel in simulated fuel grade ethanol," *Electrochim Acta*., 104, pp. 255-66 (2013).
[5] Lou, X., Yang, D., Singh, P.M. "Effect of ethanol chemistry on stress corrosion cracking of carbon steel in fuel-grade ethanol," *Corros.,* 65, pp. 785-797 (2009).
[6] Goodman, L.R., Singh, P.M. "Repassivation behaviour of X65 pipeline steel in fuel grade ethanol and its implications for the stress corrosion cracking mechanism," *Corros. Sci*. 65, pp. 238-248 (2012).
[7] Kane, R.D., Maldonado, J.G., Klein, L.J. "Stress corrosion cracking in fuel ethanol: a newly recognized phenomenon," *Proc. of NACE conference*, pp. 1-16, (2004).
[8] ASTM-D-4806-07, "Standard Specification for Denatured Fuel ethanol for Blending with Gasolines for Use as Automotive Spark-Ignition Engine Fuel," *ASTM International*, pp. 1-8 (2007).
[9] Joseph, O.O., "Chloride effects on the electrochemical degradation of micro-alloyed steel in E20 simulated fuel ethanol blend," *Res. in Phy*. **7**, pp. 1446-1451 (2017).
[10] Joseph, O.O., Loto, C.A., Sivaprasad, S., Ajayi, J.A., Tarafder, S., Role of Chloride in the Corrosion and Fracture Behavior of Micro-Alloyed Steel in E80 Simulated Fuel Grade Ethanol Environment," *Materials,* 9, pp. 463 (2016).
[11] ASTM G1-03, "Standard Practice for Preparing, Cleaning and Evaluating Corrosion Test Specimens," *ASTM International*, pp. 1-9 (2011).
[12] Yahya, S., Othman, N.K., Daud, A.R., Jalar, A., "Effect of scan rate on corrosion inhibition of carbon steel in the presence of rice straw extract - Potentiodynamic studies," *Sains Malaysiana.,* 43, pp. 1083-1087 (2014).